TEMPERATURE INFLUENCE ON THE OXYGEN AND CARBON DIOXIDE TRANSPORT IN THE HUMAN HEAD

Cyro Albuquerque Neto, cyro.albuquerque@poli.usp.br
Jurandir Itizo Yanagihara, jurandir.yanagihara@poli.usp.br
Laboratory of Environmental and Thermal Engineering (LETE)
Department of Mechanical Engineering (PME)
Escola Politécnica da Universidade de São Paulo (Poli – USP)
Cidade Universitária – São Paulo – SP – CEP 055809-900

Abstract. *The aim of this work is the analysis of the temperature influence on the oxygen and carbon dioxide transport in the human head. A dynamic model was developed for this purpose. The head is represented by a sphere with the following tissue layers: brain, bone, muscle, fat and skin. Arterial blood from the trunk flows through small vessels in equilibrium with the tissues, exchanging gases and heat. The gases are transported by the blood and tissues dissolved and chemically reacted. Metabolism takes place in the tissues, where oxygen is consumed generating carbon dioxide and heat. The skin exchanges heat with the environment by convection, radiation and evaporation. The body temperature regulation includes variations in the skin blood flow, sweat and muscle heat production by shivering, all function of the skin and internal temperature. The differential transport equations were obtained by heat and mass balances. Sphere coordinates were adopted. The discretization equations were obtained applying the finite volume method. The steady state results show the temperature, oxygen and carbon dioxide variation for several operative temperatures. Because of the negligible blood flow, the bone and fat were not considered for the gas transport analysis. In the brain, the gas variations are small and depend mostly on the arterial blood temperature from the trunk. In a cold environment, the muscle oxygen partial pressure decreases and the carbon dioxide increases because of the heat production by shivering, which consumes oxygen and produces carbon dioxide. In a warm environment, the increase of the blood flow brings more arterial oxygenated blood increasing the oxygen partial pressure. It also removes the carbon dioxide more efficiently decreasing the carbon dioxide partial pressure. For the transient analysis, the head was taken from a warm to a cold environment. The results also show that the skin and muscle gas transport are largely influenced by the temperature regulation.*

Keywords: *Bioengineering, Heat Transfer, Mass Transfer, Human head*

1. INTRODUCTION

The brain normal functioning depends on constant temperature. It also depends on oxygen availability and constant pH, which is mostly function of the carbon dioxide amount.

Models of the heat and respiratory gases have been developed around the world since the middles of the last century. The first model of the thermal system is from Pennes (1948). He applied the heat conduction equation, adding a blood perfusion term, in the human forearm. Its equation is known nowadays as the "bio-heat equation" and is largely used. Grodins et al. (1954) developed the first respiratory system model. The blood, tissues and lung were represented by compartments, where mass balances were applied. The purpose was the study of carbon dioxide regulation.

Models taking into account the interactions of heat, oxygen and carbon dioxide transport have been developed in some recent works. The model of Ji and Liu (2002) was applied to studies on the blood viscosity increases in the brain hypothermia resuscitation.

The present work is focused on the heat and gas transport in the human head, and their influences on each other. The model development is based on two previous works developed in the same laboratory. Those are the thermal system model of Ferreira (2001), and the respiratory system model of Albuquerque-Neto (2005).

2. HEAD REPRESENTATION

The human head is represented by a sphere with five layers inside. Those are the five kinds of tissues considered, based on its particular characteristics: brain, bone, muscle, fat and skin (Fig. 1).

The size of each layer depends on its volume, obtained from the detailed data of Werner and Buse (1988), for a man with 1.76 m of height and mass of 67 kg. The connective and vessel tissues were divided among the other tissues, and the volume of the neck tissues were subtracted (Ferreira, 2001). The layer volumes and their calculated external rays are in Tab. 1.

The skin exchanges heat with the environment by convection, radiation and evaporation. It depends on the environment conditions (air temperature, radiant temperature and humidity).

Arterial blood gets into the head from the trunk and neck. This blood is then distributed around the tissues inside the small vessels. Leaving the tissues, the venous blood returns to the trunk.

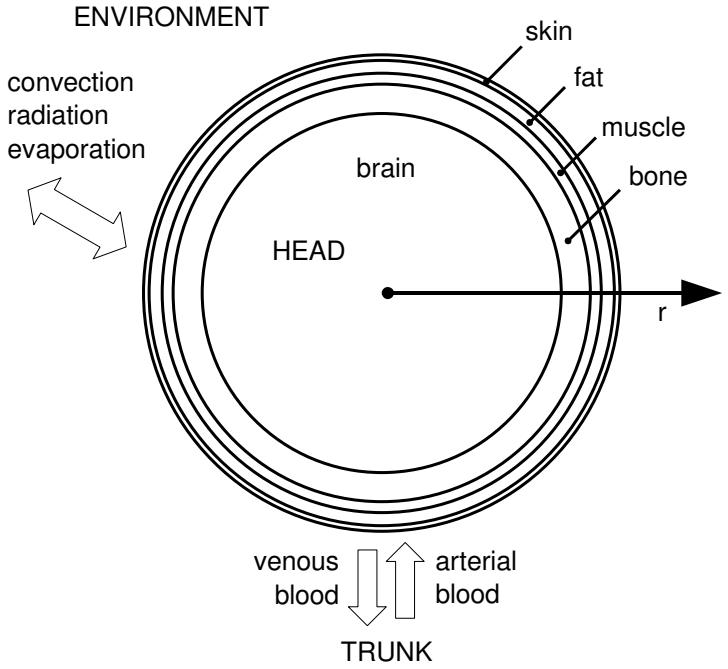

Figure 1: Head representation.

Based on the work of Chen and Holmes (1980), the blood in the small vessels is in thermal equilibrium with the tissues. Thus, the head blood volume was divided between the small and large vessels. It was considered as small vessels the terminal branch, small artery, arteriole, capillary, venule and terminal vein. All the gas transfer between tissues and blood happens in the small vessels. The tissue volume includes the blood volume present in the small vessels, which was determined for each kind of tissue based on the total volume of blood in the head, the relation between large and small vessels, and the distribution of the basal blood flow (Tab. 1).

3. TISSUES

Each tissue has its specific characteristics. The skin is in contact with the environment and has variable blood flow. The fat has low heat conductivity and blood flow. The muscle stores chemically reacted oxygen. The blood flow in the bone is negligible. The brain has high blood flow and metabolism. Table 1 presents the tissue parameters used in the present model.

Table 1: Tissue parameters.

	Skin	Fat	Muscle	Bone	Brain	
Tissue volume [1][2]	245	528	393	860	1514	cm^3
Small vessel blood volume	4.73	2.17	11.37	0.00	726.07	10^{-7} cm^3
External ray	9.45	9.23	8.71	8.28	7.12	cm
Basal blood flow [1]	362	77	543	0	9000	10^{-6} $m^3/(m^3.s)$
Density [1]	1085	920	1085	1357	1080	kg/m^3
Heat capacity [1]	3680	2300	3800	1700	3850	J/(kg.°C)
Heat conductivity [1]	0.47	0.21	0.51	0.75	0.49	W/(m.°C)
Heat production (37 °C)[1]	368	368	684	368	9472	W/m^3
Respiratory quocient [3]	0.85	–	0.85	–	1.00	
Tissue CO_2 dissociation curve slope [4]	0.0225	–	0.0315	–	0.0218	m^3/(kg.Pa)

[1] Werner and Buse (1988); [2] Ferreira (2001); [3] Mountcastle (1980); [4] Farhi and Rahn (1960)

The human body energy is generated by the oxidation of some compounds with bonds between carbon and hydrogen. CO_2, water and heat are generated as a product of that oxidation. The relation between the amount of CO_2 produced and the O_2 consumed is the respiratory quotient (RQ). The following equation relates the heat production, the O_2

consumption, and the respiratory quotient (Mountcastle, 1980):

$$\hat{\dot{q}}_t = [1.662 \times 10^7 + 5.16 \times 10^6 \, (RQ - 0.707)] \, \hat{\dot{V}}_{O_2,t} \tag{1}$$

where: $\hat{\dot{q}}_t$ = heat production [W/m^3]; RQ = respiratory quotient [m^3/m^3]; $\hat{\dot{V}}_{O_2,t}$ = tissue O_2 consumption [m^3/(m^3.s)].

The metabolic heat production depends on chemical reactions affected by temperature, which also influence the O_2 consumption and CO_2 production. The corrected heat production is calculated by the following equation, referenced to the heat production at 37 °C (Tab. 1) (Werner and Buse, 1988; Mountcastle, 1980).

$$\hat{\dot{q}}_t = \hat{\dot{q}}_{t,0} \, 2^{(T_t - 37)/10} \tag{2}$$

where: $\hat{\dot{q}}_{t,0}$ = heat production at 37 °C [W/m^3]; T_t = tissue temperature [°C].

The O_2 is stored dissolved in the tissues, and also chemically reacted with myoglobin in the muscles. The CO_2 is stored dissolved, as bicarbonate ion and as carbonate in the bone. Because of the low blood flow, the gas exchanges in the bone and fat are not considered in the present model.

The amount of dissolved gases is equal to their partial pressures multiplied by the gas solubility coefficient. The tissue solubility coefficient is difficult to be determined. For the oxygen, it is considered to be the same as the O_2 solubility in the water, 2.36×10^{-7} m^3/(m^3.Pa) at 37 °C (Altman and Dittmer, 1971).

The protein called myoglobin is used for O_2 storage in the muscle, forming the oxymyoglobin (O_2Mb). The maximum myoglobin capacity to store the gases is determined as the blood hemoglobin capacity multiplied by the relation of their molecular masses, 68000 for hemoglobin and 17600 for mioglobin (Guyton and Hall, 2006), divided by four (hemoglobin carries four molecules and myoglobin one). This relation was based on Bruce and Bruce (2003). The myoglobin concentration in the muscles is 0.0053 g/cm^3 (Coburn and Mayers, 1971). The myoglobin saturation is represented according to Schenkman et al. (1997), in function of temperature and O_2 partial pressure.

$$S_{O_2,t} = \frac{P_{O_2,t}}{P_{O_2,t} + 133.3 \, e^{(0.098 \, T_t - 2.748)}} \tag{3}$$

where: $S_{O_2,t}$ = myoglobin O_2 saturation [0–1]; $P_{O_2,t}$ = tissue O_2 partial pressure [Pa].

The CO_2 transport mechanism in the tissues, dissolved or as bicarbonate ion, is complex. A solution is to group both transport forms and treat it by an unique coefficient, the slope of the tissue CO_2 dissociation curve (Tab. 1). Therefore, the tissue CO_2 content is equal to this coefficient multiplied by the tissue CO_2 partial pressure (Farhi and Rahn, 1960).

4. BLOOD

The O_2 is transported by the blood dissolved and chemically reacted with hemoglobin. The CO_2 is transported by the blood dissolved, reacted with hemoglobin and as bicarbonate ion.

The O_2 solubility coefficient in the blood is equal to 2.93×10^{-5} m^3/(m^3.Pa) at 37 °C (Altman and Dittmer, 1971). The relation between the solubility of O_2 in the blood and water is constant in the range of corporal temperatures (Hedley-Whyte and Laver, 1964). It follows that the O_2 solubility coefficient in the blood is determined the following equation (Thomas, 1972):

$$\alpha_{O_2,bl} = 2.93 \times 10^{-5} \left[1 + \log(T_{bl}/37) + 0.00012 \, (T_{bl} - 37)^2\right] \tag{4}$$

where: $\alpha_{O_2,bl}$ = blood O_2 solubility coefficient [m^3/(m^3.Pa)]; T_{bl} = blood temperature [°C].

Most of O_2 is carried by the blood through its chemical reaction with hemoglobin. The relation between the maximum amount of O_2 with hemoglobin is 3.14 cm^3/g; and the blood hemoglobin concentration $[Hb]$ is 0.15 g/cm^3 for a normal subject (Guyton and Hall, 2006). The relation between the O_2 partial pressure and its saturation (relation between the amount of O_2 reacted and the total amount of hemoglobin) is given by a dissociation curve. It varies in function of the CO_2 amount in the blood and temperature. The oxygen saturation is obtained as proposed by Thomas (1972):

$$S_{O_2,bl} = \frac{N^4 - 15 \, N^3 + 2045 \, N^2 + 2000 \, N}{N^4 - 15 \, N^3 + 2400 \, N^2 - 31100 \, N + 2.4 \times 10^6} \tag{5}$$

$$N = 0.0075 \, P_{O_2,bl} \times 10^{[0.48 \, (pH - 7.4) - 0.024 \, (T_{bl} - 37) - 0.0013 \, BE]} \tag{6}$$

where: $S_{O_2,bl}$ = hemoglobin O_2 saturation [0–1]; $P_{O_2,bl}$ = blood O_2 partial pressure [Pa]; BE = base excess [mmol/dm^3].

CO_2 is transported by the blood dissolved, bonded with hemoglobin, and as bicarbonate ion. The amount of CO_2 depends on the hemoglobin saturation by O_2, temperature and pH. The pH is determined based on methodology from Turri (2006).

The first step to determine the total CO_2 content is to calculate the plasma CO_2 content with the Handerson-Hasselbalch equation (Douglas, Jones and Reed, 1988; Mountcastle, 1980). It is function of pH, CO_2 partial pressure, CO_2 solubility coefficient and pK' (related to the acid dissociation constant).

$$C_{CO_2,pl} = \alpha_{CO_2,pl}\, P_{CO_2,bl}\, \left[1 + 10^{(pH - pK')}\right] \tag{7}$$

where: $C_{CO_2,pl}$ = plasma CO_2 content [m^3/m^3]; $\alpha_{CO_2,pl}$ = plasma CO_2 solubility coefficient [$m^3/(m^3.Pa)$]; $P_{CO_2,bl}$ = blood CO_2 partial pressure [Pa]; pK' = negative logarithmic of the acid dissociation constant.

The CO_2 solubility coefficient and the pK' are functions of temperature and pH (Douglas, Jones and Reed, 1988).

$$\alpha_{CO_2,pl} = 0.0075\,[0,0307 + 0,00057\,(37 - T_{bl}) + 0,00002\,(37 - T_{bl})^2] \tag{8}$$

$$pK' = 0.0075\,\{6,086 + 0,042\,(7,4 - pH) + (38 - T_{bl})\,[0,00472 + 0,00139\,(7,4 - pH)]\} \tag{9}$$

The total blood CO_2 content is then calculated by the following equation (Douglas, Jones and Reed, 1988):

$$C_{CO_2,bl} = C_{CO_2,pl}\, \left[1 - \frac{2.89\, \times\, 10^{-5}\,[Hb]}{(3.352 - 0.456\, S_{O_2,bl})\,(8.142 - pH)}\right] \tag{10}$$

where: $C_{CO_2,bl}$ = blood CO_2 content [m^3/m^3].

5. TRANSPORT EQUATIONS

The application of the heat conduction equation in the tissues was first made by Pennes (1948). The equation includes metabolic heat production and the tissue blood perfusion in the small vessels. Using sphere coordinates and considering only the radial variation, this equation is:

$$\rho_t\, c_{p,t}\, \frac{\partial T_t}{\partial t} = k_t\, \frac{1}{r^2}\, \frac{\partial}{\partial r}\left(r^2\, \frac{\partial T_t}{\partial r}\right) + \dot{V}_{bl}\, \rho_{bl}\, c_{p,bl}\, (T_{ar} - T_t) + \hat{\dot{q}}_t \tag{11}$$

where: ρ_t = tissue density [kg/m^3]; $c_{p,t}$ = tissue heat capacity [J/(kg.°C)]; t = time [s]; k_t = tissue heat conductivity [W/(m.°C)]; r = ray [m]; $\dot{V}_{bl}$ = blood flow [$m^3/(m^3.s)$]; ρ_{bl} = blood density [kg/m^3]; $c_{p,bl}$ = blood heat capacity [J/(kg.°C)]; T_{ar} = arterial temperature [°C].

This equation has tree boundary conditions:

1. Symmetry in the sphere center: $\left.\dfrac{\partial T_t}{\partial r}\right|_{r=0} = 0$
2. In the tissue layer interface (tissues $t1$ and $t2$): $k_{t1}\dfrac{\partial T_{t1}}{\partial r}\Bigg|_{\text{interface}} = k_{t2}\dfrac{\partial T_{t2}}{\partial r}\Bigg|_{\text{interface}}$
3. Environment heat exchange on the surface: $-k_t\, \left.\dfrac{\partial T_t}{\partial r}\right|_{\text{surface}} = \dot{q}_{en}$

where: $\dot{q}_{en}$ = environment heat transfer [W/m^2].

Since the blood carries a considerable amount of O_2 and CO_2, the small vessel blood volume was separated from the tissue volume. The gas partial pressures are considered to be the same in the tissue and the small vessel blood. The variation of any gas partial pressure is represented by the following equation, applying mass balance principles. It takes into account the content convective variation from the arterial blood, and the gas production (or consumption).

$$\left(\frac{V_{bl}}{V_t}\, \frac{d\, C_{g,bl}}{d\, P_{g,t}} + \frac{V_t - V_{bl}}{V_t}\, \frac{d\, C_{g,t}}{d\, P_{g,t}}\right) \frac{d\, P_{g,t}}{d\, t} = \dot{V}_{bl}\, (C_{g,ar} - C_{g,bl}) + \hat{\dot{V}}_{g,t} \tag{12}$$

where: V_{bl} = small vessel blood volume [m^3]; V_t = tissue volume [m^3]; g = gas [O_2 or CO_2]; $C_{g,bl}$ = small vessel blood g content [m^3/m^3]; $P_{g,t}$ = tissue g partial pressure [Pa]; $C_{g,t}$ = tissue g content [m^3/m^3]; $C_{g,ar}$ = arterial blood g content [m^3/m^3]; $\hat{\dot{V}}_{g,t}$ = tissue g production [$m^3/(m^3.s)$].

The relation between the blood and tissue partial pressures and their contents were described in the last two sections.

The density of the blood is 1059 kg/m^3, and the heat capacity is 3850 J/(kg.°C) (Werner and Buse, 1988).

6. ENVIRONMENT

In the contact between the skin and the environment happens heat exchange by convection, radiation and evaporation. The total environment heat exchange is the sum of these tree processes. The convection and radiation can be considered together in function of the surface tissue temperature, an operative temperature, and a combined heat transfer coefficient (ASHRAE, 2005):

$$\dot{q}_c + \dot{q}_r = h\,(T_{ts} - T_o) \tag{13}$$

$$h = h_c + h_r \tag{14}$$

$$T_o = \frac{h_r\,\bar{T}_r + h_c\,T_a}{h_r + h_c} \tag{15}$$

where: $\dot{q}_c$ = convection heat transfer [W/m^2]; $\dot{q}_r$ = radiation heat transfer [W/m^2]; h = combined heat transfer coefficient [W/(m^2.°C)]; T_{ts} = tissue surface temperature [°C]; T_o = operative temperature [°C]; h_r = radiation heat transfer coefficient [W/(m^2.°C)]; $\bar{T}_r$ = average radiant temperature [°C]; h_c = convection heat transfer coefficient [W/(m^2.°C)]; T_a = air temperature [°C].

The evaporation is determined multiplying the maximum evaporation capacity, when the skin is totally wet, by a fraction of wet surface, equal to 0.06 in the absence of sweat. As well as the convection and radiation, the amount of heat exchanged by evaporation take into account a heat transfer coefficient and the difference between the water vapour partial pressure of the skin surface and the environment (ASHRAE, 2005).

$$\dot{q}_e = w\,h_e\,(P_{w,ts} - \phi_a\,P_{w,a}) \tag{16}$$

where: $\dot{q}_e$ = evaporation heat transfer [W/m^2]; w = wet surface fraction [0–1]; h_e = evaporation heat transfer coefficient [W/(m^2.Pa)]; $P_{w,ts}$ = skin surface water vapour partial pressure [Pa]; ϕ_a = air relative humidity [0–1]; $P_{w,a}$= air water vapour partial pressure [Pa].

The convection heat transfer coefficient for the head is equal to 3.6 W/(m^2.°C), and the radiation heat transfer coefficient is equal to 4.1 W/(m^2.°C) (Dear et al., 1997). The evaporation heat transfer coefficient was determined by Ferreira (2001) by a heat and mass transfer analogy; it is equal to 0.059 W/(m^2.Pa).

7. REGULATION

The temperature regulation of the human body depends on three mechanisms: skin blood flow variation, sweat, and shivering. They vary in function of the internal and skin temperature. Those mechanisms are represented by experimental models largely used in the literature. The skin blood flow, the wet fraction surface, and the muscle heat generation by shivering is obtained respectively by Savage and Brengelmann (1996), Nadel, Bullard and Stolwijk (1971), and Gordon, Roemer and Horvath (1976). Ferreira (2001) changed the form of these three models, representing the equations by coefficients multiplied by the difference between the tissue temperature (internal or skin) and a reference temperature. New coefficients were obtained using a complete human body thermal model. Those were adopted in the present work.

The internal and skin reference temperature is obtained when the human body is in a neutral condition, meaning that the controllers are not activated, when the operative temperature is 30 °C and the relative humidity is 50% (Ferreira, 2001; Mountcastle, 1980). The internal temperature is represented by the average brain temperature. The reference temperatures were obtained from simulation of the present model. They are equal to 36.84 °C for the brain and 34.52 °C for the skin.

The skin blood flow is determined by the following equation, limited from 330×10^{-6} to 3800×10^{-6} m^3/(m^3.s):

$$\dot{V}_{bl,sk} = 180 \times 10^{-6}\,(\bar{T}_{sk} - 34.52) + 1800 \times 10^{-6}\,(\bar{T}_{br} - 36.84) + 362 \times 10^{-6} \tag{17}$$

where: $\dot{V}_{bl,sk}$ = skin blood flow [m^3/(m^3.s)]; $\bar{T}_{sk}$ = average skin temperature [°C]; $\bar{T}_{br}$ = average brain temperature [°C].

The first step for the determination of the sweat effect is to calculate the evaporation heat transfer on the skin in function of the brain and skin temperatures:

$$\dot{q}_e = [11\,(\bar{T}_{sk} - 34.52) + 100\,(\bar{T}_{br} - 36.84)]\,e^{(\bar{T}_{sk} - 34.52)/10} \tag{18}$$

The wet surface fraction is then determined by the following equations, limited from 0.06 to 1:

$$w = 0.06 + 0.94\,\dot{q}_e/\dot{q}_{e,max} \tag{19}$$

where: $\dot{q}_{e,max}$ = maximum evaporation heat transfer [W/m^2], from equation (16).

The increase in the muscle heat production by shivering is determined by the following equation, limited from 0 to 15500 W/m^3:

$$\Delta\hat{\dot{q}}_m = 1446\,(\bar{T}_{sk} - 34.52) + 9036\,(\bar{T}_{br} - 36.84) \tag{20}$$

where: $\Delta\hat{q}_m$ = muscle heat production variation [W/m^3].

As the muscle heat production increases, the oxygen consumption, the carbon dioxide production, and the blood flow also increase. The muscle blood flow variation can be related to the oxygen consumption variation (interpolated from Guyton and Hall, 2006):

$$\Delta\dot{V}_{bl,m} = 7.6\,\Delta\dot{V}_{O_2,m} \tag{21}$$

where: $\Delta\dot{V}_{bl,m}$ = muscle blood flow variation [m^3/(m^3.s)]; $\Delta\dot{V}_{O_2,m}$ = muscle oxygen consumption variation [m^3/(m^3.s)].

8. SOLUTION

The heat transport equation (11) was solved using the finite volume method, according to Pantankar (1980). First the head ray was divided into points representing each control volume. Between those points are the control volume faces. The size of each control volume varies depending on its tissue layer. The faces coincide with the tissue interfaces. The mass transport equation (12) is also solved for each control volume.

The heat discretization equation was obtained integrating each term of the heat transport equation (multiplied by $r^2\,\sin\theta$) with respect to time and each spherical coordinate: r (from the east to west face), θ (from 0 to π), and ϕ (from 0 to 2π). The obtained discretization equation is function of the center point (P), the east and west point (E and W), and the east and west face (e and w):

$$a_P\,T_{t,P} = a_E\,T_{t,E} + a_W\,T_{t,W} + b \tag{22}$$

$$a_E = 4\pi\,k_{t,e}\,r_e^2/(\delta r)_e \tag{23}$$

$$a_W = 4\pi\,k_{t,w}\,r_w^2/(\delta r)_w \tag{24}$$

$$a_P^0 = \rho_t\,c_t\,\Delta V/\Delta t \tag{25}$$

$$b = (\dot{V}_{bl}\,\rho_{bl}\,c_{p,bl}\,T_{ar} + \hat{q}_t)\,\Delta V + a_P^0\,T_{t,P}^0 \tag{26}$$

$$a_P = a_E + a_W + a_P^0 + \dot{V}_{bl}\,\rho_{bl}\,c_{p,bl}\,\Delta V \tag{27}$$

where: $T_{t,P}$ = center point tissue temperature [°C]; $T_{t,E}$ = east point tissue temperature [°C]; $T_{t,W}$ = west point tissue temperature [°C]; $k_{t,e}$ = east tissue heat conductivity [W/(m.°C)]; r_e = east face ray [m]; $(\delta r)_e$ = center to east point distance [m]; $k_{t,w}$ = west tissue heat conductivity [W/(m.°C)]; r_w = west face ray [m]; $(\delta r)_w$ = center to west point distance [m]; ΔV = control volume [m^3]; Δt = time step [s]; $T_{t,P}^0$ = last center point tissue temperature [°C].

The interface conductivity is determined by an approach described by Patankar (1980), based on the heat flux continuity.

A computational program based on C++ language was developed in order to solve the equations in the steady state and transient conditions. For the steady state, it was used a successive approximation method. For the transient solution a explicit scheme was used.

The number of control volumes in each tissue layer was determined from tests aiming a good approximation. The brain was so divided in 20 control volumes. The others tissue layers were divided in 10 control volumes each.

9. RESULTS

Figure 2 shows the steady state tissue temperature variation along the head ray, from the center to the surface, for several operative temperatures. The vertical lines inside the graph are the tissue layer interfaces.

The skin has the smallest temperature, because of its contact with the environment. The fat characteristic as a thermal insulating material is showed by its large temperature variation along the layer. The increase of the heat production by shivering in the muscle when the operative temperature is low prevents large internal temperature variations. When the operative temperature is high, the increase in the sweat and skin blood flow helps the maintaining of a constant internal temperature.

The brain has high blood flow. Because of that, the brain temperature is much influenced by the arterial blood temperature coming from the trunk, here set as 36.6 °C. The determination of the arterial blood temperature variation needs a complete human body model. As an example of this effect, the Fig. 3 shows the tissue temperature variation along the head ray, for three different arterial temperatures, and operative temperature of 30 °C. The brain temperature variation is clearly observed.

Figure 4 shows the steady state O_2 partial pressure variation in the brain, muscle and skin layers, for several operative temperatures (same as Fig. 2). The bone and fat were not considered in the gas analysis because of their negligible blood flow. The dots of the graph represents each tissue control volume.

The constant O_2 partial pressure in the brain is reflection of the constant temperature. The muscle presents a small O_2 partial pressure variation for operative temperatures of 30 and 40 °C. However, for operative temperatures of 10 and 20 °C

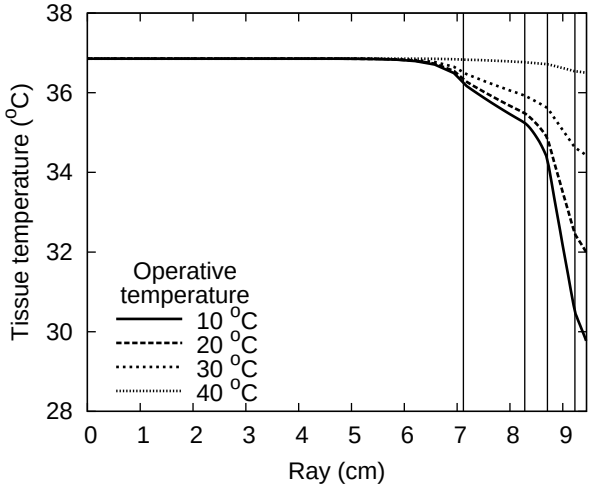

Figure 2: Steady state tissue temperature along the head ray for different operative temperatures.

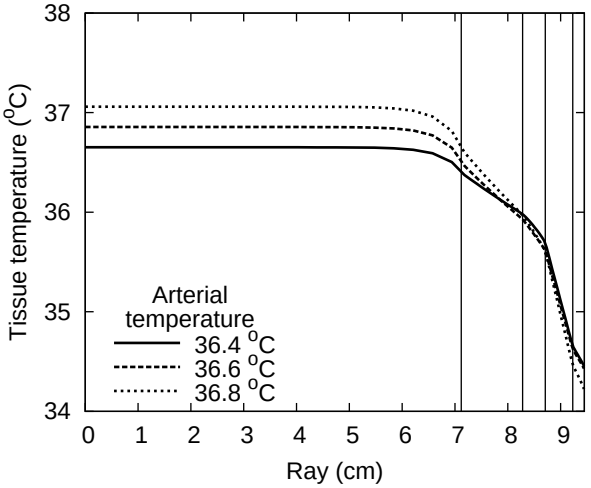

Figure 3: Steady state tissue temperature along the head ray for different arterial blood temperatures.

the O_2 partial pressure decreases. This is result of the O_2 consumption increase by shivering. In the skin, a larger variation can be noticed when the temperature is 40 °C. This effect is also result of the regulation mechanism. The increase of the skin blood flow brings more oxygenated arterial blood, which increases the O_2 content in the skin.

The CO_2 partial pressure variation for several operative temperatures is showed in Fig. 5. The more considerable variations of the CO_2 partial pressure are also regulation effects. For low operative temperatures, the CO_2 partial pressure is higher because of the CO_2 production by shivering. In the skin, the CO_2 partial pressure increases as the operative temperature increases until 30 °C. However, when the operative temperature is equal to 40 °C, the CO_2 partial pressure decreases. This fact occurs because of the increase in the CO_2 removal as the blood flow increases.

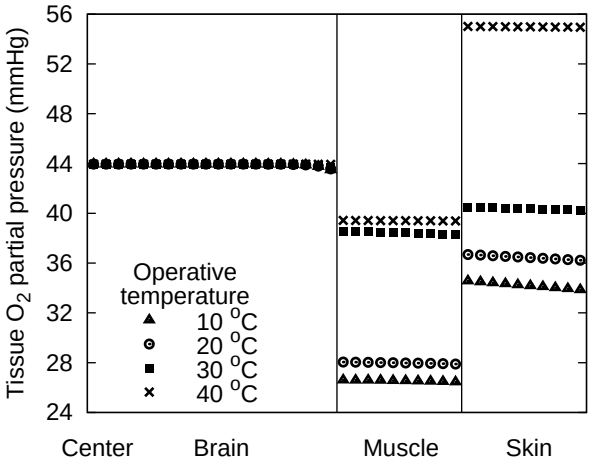

Figure 4: Steady state tissue O_2 partial pressure in the brain, muscle and skin layers for different operative temperatures.

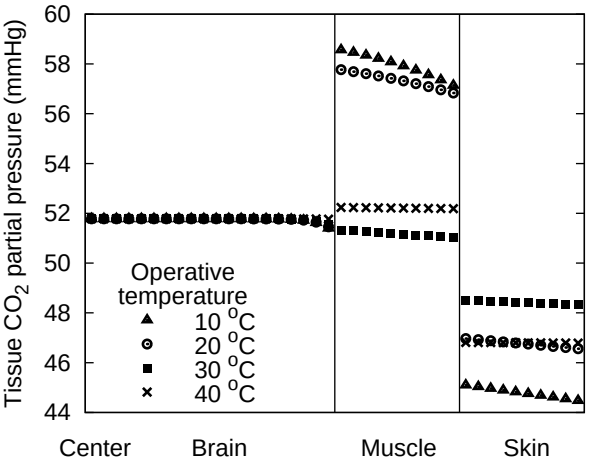

Figure 5: Steady state tissue CO_2 partial pressure in the brain, muscle and skin layers for different operative temperatures.

For the transient analysis, it was considered a situation in which the human head is taken from the operative temperature of 40 °C to 10 °C. These temperatures were chosen because, between them, all the regulation mechanisms are activated.

Figure 6 shows the average temperature of each tissue layer. The simulation starts with the head steady state condition when the operative temperature is 40 °C. Just after the beginning of the simulation, the operative temperature is set to 10 °C. After one hour of simulation, the tissue temperatures almost reach a new steady state. The tissue temperature variation is larger as closer the tissue is to the surface.

The controlled variables are showed on Fig. 7. These are the wet surface fraction, the skin blood flow, and the muscle heat production by shivering, all function of the internal and skin temperature. The variables were normalized between their up and down limit, so their variation is from 0 to 1. In the beginning of the simulation, the skin blood flow and

the sweat are activated. After about 10 minutes, these mechanisms are set off, and the muscle starts to produce heat by shivering.

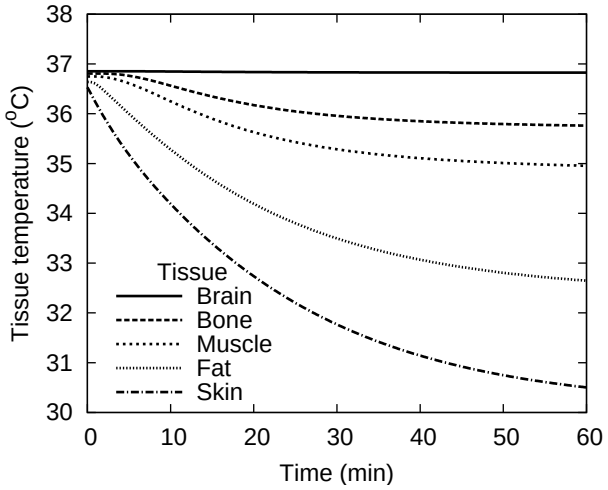

Figure 6: Transient average tissue temperature from 40 °C to 10 °C.

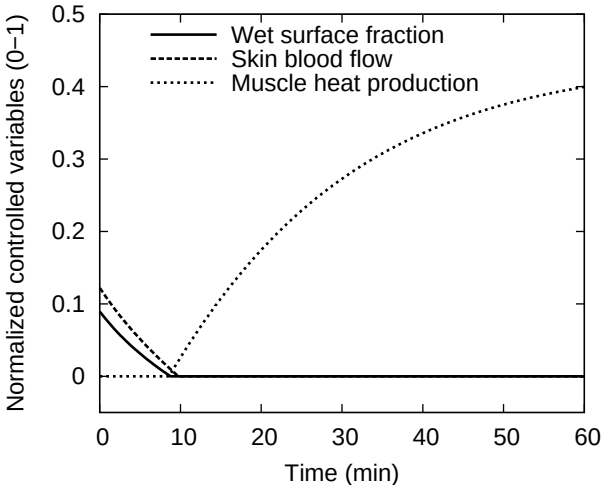

Figure 7: Transient normalized controlled variables from 40 °C to 10 °C.

The average tissue O_2 and CO_2 partial pressures are shown in Fig. 8 and Fig. 9 respectively. It can be noticed that the main variations follow the regulation mechanisms.

The muscle O_2 and CO_2 partial pressures are almost constant before the first 10 minutes of simulation. After that, the heat production by shivering starts. It results in an increase of the O_2 consumption and the CO_2 production. Consequently, the muscle O_2 partial pressure decreases and the muscle CO_2 partial pressure increases.

In the skin, the O_2 partial pressure drops down while the regulation by sweat and skin blood flow is decreasing. At this stage, the skin is been more oxygenated by the high blood flown from the trunk. After that, the O_2 partial pressure continues to decrease slowly. The CO_2 partial pressure variation is smaller. First it increases reflecting the decrease of the CO_2 removal from the skin blood flow. Then the CO_2 partial pressure decreases following the decrease of the tissue temperature.

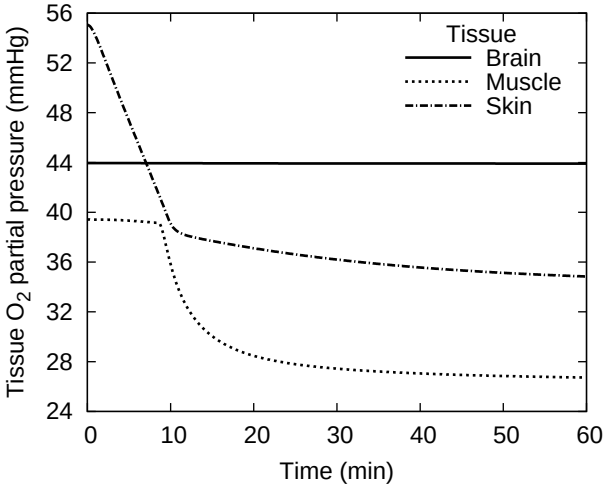

Figure 8: Transient average tissue O_2 partial pressure from 40 °C to 10 °C.

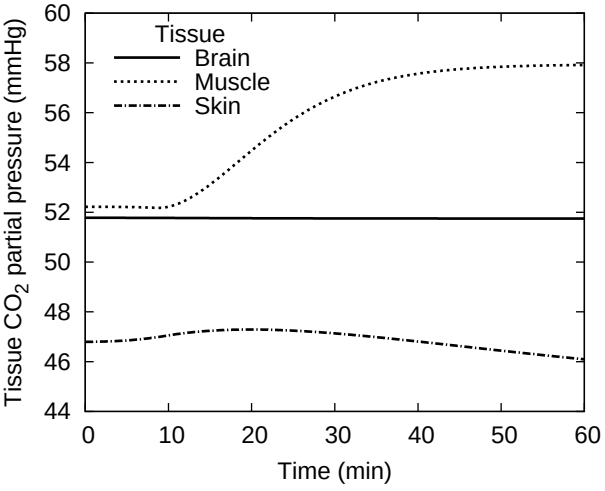

Figure 9: Transient average tissue CO_2 partial pressure from 40 °C to 10 °C.

10. CONCLUSION

In this work, a model of the oxygen, carbon dioxide and heat transport in the human head was developed. The purpose was the study of the temperature influence on the gas transport. The head was represented by a sphere with tissue layers (brain, bone, muscle, fat and skin). Blood pass through the tissues in the small vessels and exchanges gases and temperature. The gases are transported dissolved and reacted with the blood and tissues. On the skin contact

with the environment happens convection, radiation and evaporation heat exchanges. The regulation mechanisms include the sweat, skin blood flow and shivering. Transport equations were developed and solved in steady state and transient conditions.

The results showed that the gas variations in the brain are mostly depended on the blood conditions coming from the trunk. On the other hand, the muscle and skin gas variations are largely influenced by the regulation mechanisms. In a warm environment, the skin blood flow increases, which brings more oxygen from the arterial blood and removes more carbon dioxide. In a cold environment, the increase in the muscle heat generation by shivering increases the oxygen consumption and the carbon dioxide production.

In conclusion, the present model showed that the thermal regulation and the arterial blood characteristics have considerable influence on the oxygen and carbon dioxide transport.

11. REFERENCES

Albuquerque-Neto, 2005, "Um modelo do transporte de monóxido de carbono no sistema respiratório do corpo humano", Masther Thesis, Escola Politécnica, Universidade de São Paulo, São Paulo, Brazil, 129 p. (in portuguese)

Altman, P.L., Dittmer, D.S., 1971, "Biological Handbooks: Respiration and circulation", Federation of American Societies for Experimental Biology, Bethesda, USA, 930 p.

ASHRAE – American Society of Heating, Refrigerating and Air-Conditioning Engineers, 2005, "Handbook, Fundamentals", Atlanta, USA.

Bruce, E.N., Bruce, M.C., 2003, "A multicompartment model of carboxyhemoglobin and carboxymyoglobin responses to inhalation of carbon monoxide", Journal of Applied Physiology, Vol.95, No.3, pp. 1235-1247.

Chen, M.M., Holmes, K.R., 1980, "Microvascular contributions in tissue heat transfer", Annals of the New York Academy of Sciences, Vol.335, pp. 137-150.

Coburn, R.F., Mayers, L.B., 1971, "Myoglobin O_2 tension determined from measurements of carboxymyoglobin in skeletal muscle", American Journal of Physiology, Vol.220, No.1, pp. 66-74.

Dear, R.J., Arens, E., Hui, Z., Oguro M., 1997, "Convective and radiative heat transfer coefficients for individual human body segments", International Journal of Biometeorology, Vol.40, No.3, pp. 141-156.

Douglas, A.R., Jones, N.L., Reed, J.W., 1988, "Calculation of whole blood CO_2 content", Journal of Applied Physiology, Vol.65, No.1, pp. 473-477.

Farhi, L.E., Rahn, H., 1960, "Dynamics of changes in carbon dioxide stores", Anesthesiology, Vol.21, pp. 604-14.

Ferreira, M.S., 2001, "Um modelo do sistema térmico do corpo humano", Ph.D. Thesis, Escola Politécnica, Universidade de São Paulo, São Paulo, Brazil, 166 p. (in portuguese)

Gordon, R.G., Roemer, R.B., Horvath, S.M., 1976, "A mathematical model of the human temperature regulatory system - transient cold exposure response", IEEE Transactions on Biomedical Engineering, Vol.23, pp. 434-444.

Grodins, F.S., Gray, J.S., Schroeder, K.R., Norins, A.L., Jones, R.W., 1954, "Respiratory responses to CO_2 inhalation. A theoretical study of a nonlinear biological regulator", Journal of Applied Physiology, Vol.7, No.3, pp. 283-308.

Guyton, A.C., Hall, J.E., 2006, "Textbook of medical physiology", Ed. Saunders, 11.ed, Philadelphia, USA, 1104 p.

Hedley-Whyte, J., Laver, M.B., 1964, "O_2 solubility in blood and temperature correction factors for P_{O_2}", Journal of Applied Physiology, V.19, No.5, pp. 901-906.

Ji, Y., Liu, J., 2002, "Numerical studies on the effect of lowering temperature on the oxygen transport during brain hypothermia resuscitation", Computers in Biology and Medicine, Vol.32, No.6, pp. 495-514.

Nadel, E.R., Bullard, R.W., Stolwijk, J.A.J., "Importance of skin temperature in the regulation of sweating", Journal of Applied Physiology, Vol.31, No.1, pp. 80-87.

Mountcastle, V.B., 1980, "Medical physiology", Ed. C.V. Mosby Company, 14.ed, St. Louis, USA, 2192 p.

Patankar, S.V., 1980, "Numerical heat transfer and fluid flow", Ed. Hemisphere Publishing Corporation, Washington, USA, 210 p.

Pennes, H.H., 1948, "Analysis of tissue and arterial blood temperatures in the resting human forearm", Journal of Applied Physiology, Vol.1, No.2, pp. 93-122.

Savage, M.V., Bregelmann, G.L., "Control of skin blood flow in the neutral zone of human body temperature regulation", Journal of Applied Physiology, Vol.80, No.4, pp. 1249-1257.

Schenkman, K.A., Marble, D.R., Burns, D.H., Feigl, E.O., 1997, "Myoglobin oxygen dissociation by multiwavelenght spectroscopy", Journal of Applied Physiology, Vol.82, No.1, pp. 86-92.

Thomas, L.J., 1972, "Algorithms for selected blood acid-base and blood gas calculations", Journal of Applied Physiology, Vol.33, No.1, pp.154-158.

Turri, F., 2006, "Análise teórico-experimental do transporte de oxigênio e gás carbônico em oxigenadores de sangue", Ph.D. Thesis, Escola Politécnica, Universidade de São Paulo, São Paulo, Brazil, 221 p. (in portuguese)

Werner, J., Buse, M., 1988, "Temperature profiles with respect to inhomogeneity and geometry of the human body", Journal of Applied Physiology, Vol.65, No. 3, pp. 1110-1118.

12. Responsibility notice

The authors are the only responsible for the printed material included in this paper